Finite element modeling to analyze TEER values across silicon nanomembranes

Tejas S. Khire, Barrett J. Nehilla, Jirachai Getpreecharsawas, Maria E. Gracheva, Richard E. Waugh & James L. McGrath

Biomedical Microdevices
BioMEMS and Biomedical Nanotechnology

ISSN 1387-2176
Volume 20
Number 1

Biomed Microdevices (2018) 20:1-11
DOI 10.1007/s10544-017-0251-7

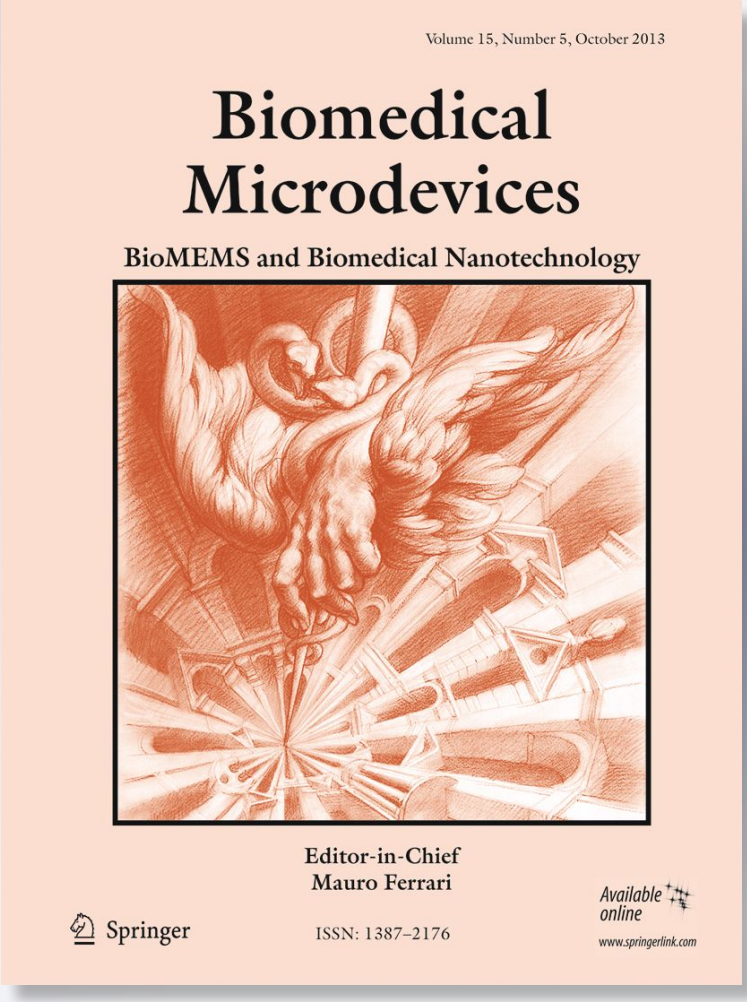

Springer

Biomed Microdevices (2018) 20:11
https://doi.org/10.1007/s10544-017-0251-7

Finite element modeling to analyze TEER values across silicon nanomembranes

Tejas S. Khire[1] · Barrett J. Nehilla[1,2] · Jirachai Getpreecharsawas[1] · Maria E. Gracheva[3] · Richard E. Waugh[1] · James L. McGrath[1]

Abstract

Silicon nanomembranes are ultrathin, highly permeable, optically transparent and biocompatible substrates for the construction of barrier tissue models. Trans-epithelial/endothelial electrical resistance (TEER) is often used as a non-invasive, sensitive and quantitative technique to assess barrier function. The current study characterizes the electrical behavior of devices featuring silicon nanomembranes to facilitate their application in TEER studies. In conventional practice with commercial systems, raw resistance values are multiplied by the area of the membrane supporting cell growth to normalize TEER measurements. We demonstrate that under most circumstances, this multiplication does not 'normalize' TEER values as is assumed, and that the assumption is worse if applied to nanomembrane chips with a limited active area. To compare the TEER values from nanomembrane devices to those obtained from conventional polymer track-etched (TE) membranes, we develop finite element models (FEM) of the electrical behavior of the two membrane systems. Using FEM and parallel cell-culture experiments on both types of membranes, we successfully model the evolution of resistance values during the growth of endothelial monolayers. Further, by exploring the relationship between the models we develop a 'correction' function, which when applied to nanomembrane TEER, maps to experiments on conventional TE membranes. In summary, our work advances the the utility of silicon nanomembranes as substrates for barrier tissue models by developing an interpretation of TEER values compatible with conventional systems.

Keywords Silicon nanomembranes · Microfluidics · Trans endothelial electrical resistance (TEER) · Coculture systems · Finite element analysis

1 Introduction

There is a need for cell culture systems that faithfully mimic the physiological response of human tissues. These systems aim to overcome enormous inefficiencies in the drug discovery pipeline (Sutherland et al. 2013) by developing platforms that have higher throughput than existing animal models, and are more reliable predictors of human tissue behaviors (Seok et al. 2013). There are now dozens of examples of microphysiological systems (MPS) or 'tissue chips' that use artificial membranes to pattern cells as barriers between apical and basal compartments of the device (Nehilla et al. 2014; Walter et al. 2016; Henry et al. 2017; Ferrell et al. 2010; Agrawal et al. 2010; Wang et al. 2017). Such designs allow investigators to create

Funds supporting this research were provided by the US Public Health Service under NIH grant number 5R01 HL125265

Tejas S. Khire and Barrett J. Nehilla contributed equally to this paper

Electronic supplementary material The online version of this article (https://doi.org/10.1007/s10544-017-0251-7) contains supplementary material, which is available to authorized users.

✉ James L. McGrath
jmcgrath@bme.rochester.edu

[1] Biomedical Engineering, University of Rochester, Goergen Hall, Rochester, NY 14627, USA

[2] Nexgenia Inc., 454 North 34th St., Seattle, WA 98103, USA

[3] Department of Physics, Clarkson University, 277 Science Center, Potsdam, NY 13699, USA

Published online: 05 January 2018

mimetic devices that can be used to understand the role of barrier tissues in diseases and to study the permeation of pharmacological drugs to underlying tissue. Despite the ubiquity of membranes in MPS devices, relatively little attention has been paid to the role that membrane properties play in the tissue models. In principle, the permeability, pore size, thickness, stiffness, and surface chemistry of an artificial membrane can each affect the accuracy of a physiological mimic. The need for optically transparent membranes that enable imaging assays further complicates the situation. The most popular forms of artificial membrane in MPS systems have been track-etched polycarbonate (TE-PC) or polyethylene terephthalate (TE-PET) membranes. These membranes are available stand-alone and also are the component of the commercial 'Transwell® inserts' (hereafter simply referred as 'transwell' or 'transwell inserts') that have been used for decades in biomedical research. The membranes are much thicker (~10 um) than basement membranes and perform poorly in microscopy because of light scattering by pores. 'Transparent' versions of these membranes have very low porosity (< 1%) making them even less physiologically relevant (Walter et al. 2016).

Our laboratories have pioneered the development of ultrathin silicon-based membranes for a variety of applications including cell culture (Striemer et al. 2007; Nehilla et al. 2014; Agrawal et al. 2010; DesOrmeaux et al. 2014; Mazzocchi et al. 2014; Carter et al. 2017; Casillo et al. 2017). The thickness of these 'nanomembranes' is between 15 nm and 400 nm with porosities as high as 30%. Their thinness makes nanomembranes far better mimics of native basement membranes (100 nm thickness *in vivo*) (Tanner 2012; Kelley et al. 2014) than TE membranes. Also, nanomembranes exhibit a permeability to small molecules that is indistinguishable from free diffusion (Snyder et al. 2011; Ishimatsu et al. 2010). Silicon nanomembranes also have glass-like optical qualities enabling superior imaging, and the silicon platform enables facile and robust bonding to silicone/polydimethylsiloxane (PDMS) materials using oxygen-plasma and UV-ozone treatments that is difficult to achieve using the chemically inert TE-PET/TE-PC membranes. Thus, silicon nanomembranes are a superior choice to TE membranes for the construction of barrier tissue models *in vitro*.

This report focuses broadly on the assumptions, conventions and sources of errors involved during the interpretation of trans endothelial electrical resistance (TEER) values from customized microfluidic systems for studying barrier properties, and more specifically on one of the challenges involved in the use of silicon nanomembranes to study barrier function. We present a brief background on *in vivo* methods for measuring vascular permeability from which the the conventions used for *in vitro* measurements originate. Using Finite Element Analysis (FEA), we then develop electrical models of 'transwell' systems employing silicon nanomembranes and conventional TE membranes. The modeling results demonstrate that the limited active (permeable) areas of silicon nanomembranes add significant baseline electrical resistance even though the membranes themselves add negligible resistance. Analyzing the TEER values from parallel cell-culture experiments of brain endothelial cells (bEnd.3), we illustrate how the FEA models relate nanomembrane-TEER values to values from TE-membranes. This conversion is needed because the abundant literature from traditional device-membrane formats have resulted in rubrics that are often used to interpret barrier function. Using the model conversion, we show that bEnd.3 barrier values are comparable when grown on silicon nanomembranes vs. TE membranes, despite large differences in the raw resistance values.

2 *In vivo* characterization of endothelial permeability: standards and conventions

The conventions for reporting TEER values in cell culture studies originate in classic experiments on blood vessels in the brain of live frogs (Crone and Olesen 1982; Crone and Christensen 1981). *In vivo* electrical impedance measurements of the frog blood-brain-barrier is a gold standard in the field of (cerebral) vascular biology (Crone and Olesen 1982). In these experiments, two pairs of electrodes are introduced in the isolated superficial brain capillary of the live animal, one pair for current injection and other for recording the changes in electric potential. The current pulse travels through the solution (blood) within the capillary, while simultaneously leaking through the porous capillary wall. This geometry (Fig. 1) is analyzed using traditional cable theory (Eisenberg and Johnson 1970).

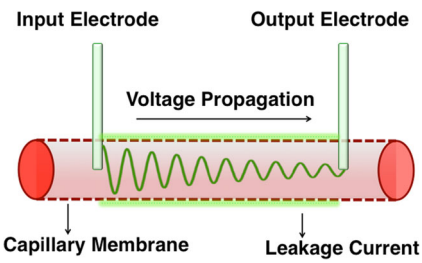

Fig. 1 The voltage drop across the two electrodes can be used to understand the ionic permeability of the blood vessel. The magnitude of signal lost is proportional to the area of the membrane between the electrodes, the electrical conductivity of the membrane bilayer, and the electrical resistivity of blood. For the sake of visual clarity, only one set of electrodes has been shown

Briefly, according to cable theory, the signal decay follows a simple exponential assuming the ionic permeability is constant along the measured vessel:

$$V(x) = V(0)e^{(-x/\lambda)} \quad (1)$$

where x is the distance from the source electrode along the axis of the capillary, and λ is the length constant that describes how rapidly the potential decays. The membrane resistance R_m is related to the internal resistance of the capillary r_i through the length constant according to:

$$R_m = r_i \cdot \lambda^2 \cdot 2\pi a \quad (2)$$

where a is the radius of the capillary (Crone and Olesen 1982; Eisenberg and Johnson 1970). r_i is determined by dividing the resistivity of the blood by the capillary cross-section area (hence Ω/cm). Thus R_m is reported in Ω·cm^2 (and not *just* Ω). This is appropriate since the loss of ionic species occurs *over* the surface of a capillary-wall and not *at* a singular location.

In vitro measurements of cellular barrier properties also employ 4-probe electrodes for the measurement of electrical resistance. Typically a low frequency, low amplitude alternating current, I, is applied across the cell-membrane barrier, and the corresponding potential drop, V, is recorded. The resistance, R, is calculated using Ohm's law: $R = V/I$, where root mean square (RMS) values are used for V and I. However, since transwell inserts are commercially available in different sizes with membrane area ranging from 0.33 cm^2 to 4.7 cm^2, the resistance values are 'normalized' by multiplying the resistance with the effective membrane area, thus reporting final TEER in Ω·cm^2. This normalization gives transwell TEER measurements the same units as *in vivo* measurements of vascular membrane resistance, even though the two experimental set-ups use different operating principles. Thus, the use of electrical resistance values from living frog brain capillaries (or other similar *in vivo* studies) as a gold standard for tissue culture measurements on endothelial cells is questionable.

The practice of normalizing tissue culture resistance values with the membrane area enables comparisons between measurements in different sized transwell systems only if the current density remains uniform across the entire device geometry as required for the straightforward application of Ohm's law. We illustrate that this assumption is not true for most transwell set-ups because of the non-uniform current distribution across the membrane (Section 4.1). Furthermore, this assumption is clearly violated for silicon nanomembranes, which have a limited active membrane area near the center of an impermeable chip. Naive 'normalization' by multiplying resistance with area results in erroneous TEER values, and make it impossible to compare barrier function between different systems. Therefore, we have developed a mapping or 'correction' function that allows for the conversion of TEER values obtained from silicon nanomembranes' systems to the commonly reported values for commercial transwell systems. In this way, TEER data acquired with nanomembranes can be related to the rich literature on *in vitro* barrier function that has been built almost exclusively using commercial transwells.

3 Materials and methods

3.1 Fabrication of silicon nanomembranes and transwell assembly

Porous nanocrystalline silicon (pnc-Si) samples were fabricated as described previously (Striemer et al. 2007) with the nanoporous membranes only 30 nm thick. Photolithography masks constrained the free-standing membrane area to comprise two 2 x 0.1 mm rectangular slits. Before assembling transwells, the pnc-Si samples were thermally treated at 1000°C for 5 minutes in a Surface Science Integration Rapid Thermal Processing (RTP) system (El Mirage, AZ). The RTP treatment significantly delays the biodegradation rate of pnc-Si (Agrawal et al. 2010). Pnc-Si samples were secured in custom polypropylene housings (Harbec Plastics, Inc., Ontario, NY) with a biocompatible O-ring to form pnc-Si transwells (Nehilla et al. 2014). The pnc-Si transwells were autoclaved before use. It is important to note that while the entire cross-sectional area of the silicon nanomembrane is available for cell growth, only the free standing area is permeable.

3.2 Effects of membrane geometry on baseline TEER values

Commercially available transwell inserts of different sizes (6-, 12-, and 24-well) featuring TE membranes were used for this study. Additionally, different active area geometries were engineered on the 12-well transwell by using wide annular silicone gaskets to cover the membrane and expose different percentages of the TE membrane in the center for permeation. In this way, we were able to simulate the active area of nanomembranes. The transwells were submerged in 1x cell medium per recommended volumes, and resistance was measured using the STX2 'chopstick' electrodes connected to EVOM Epithelial VoltOhmeter [World Precision Instruments (WPI) Inc., Sarasota, FL]. Four transwells were tested for each configuration, and 3 measurements per transwell corresponding to 3 different access-locations in the transwell.

3.3 Cell culture

Cell culture studies were performed with the mouse brain endothelial cell line 'bEnd.3' (ATCC, Manassas, VA). The bEnd.3 cells (passages 8-17) were grown in DMEM media with 1% penicillin/streptomycin, 1X non-essential amino acids and 10% FBS. The bEnd.3 cells were seeded at 50000 cells/cm^2 and grown on the bottom surface of transwells. All the cell cultures were maintained in an humidified incubator at 37°C with 5% CO_2.

3.4 Evolution of TEER values in cell culture

Barrier function of cell monolayers was assessed by measuring the electrical resistance across the transwell membranes. An EVOM Epithelial Voltohmeter connected to an EndOhm-6 (also referred as 'EndOhm') culture cup (WPI Inc., Sarasota, FL) was used for these studies. The EndOhm chamber generates a more uniform electric field as compared to the STX2 'chopstick' electrodes, and measures more accurate TEER values. Day 0 measurements were acquired before seeding cells to obtain baseline values for each transwell device, and then the TEER was measured every 2-3 days thereafter.

3.5 COMSOL simulations

All the experimental TEER measurements of barrier function were performed using an EndOhm cup for 24-well insert. The entire geometry of the EndOhm cup assembled with both commercial transwells and custom designed transwells was modeled in COMSOL Multiphysics (hereafter referred as 'COMSOL') using suitable 2D axiosymmetric and 3D models [Fig. 2]. A transwell insert consisted of a permeable membrane (TE or pnc-Si) with cells growing either on the top or bottom of the membrane, and the entire volume was filled with conducting cell medium. The conductivity (K) of the cell medium was 1.5 S/m as measured experimentally using conductivity measurement probes. The superposition principle allowed us to estimate the conductivity of the TE membrane by suitably multiplying its porosity with the cell medium conductivity; thus a 0.5% porosity membrane will be modeled as a layer with conductivity equivalent to 0.005*1.5 = 0.0075 S/m. For the pnc-Si membrane, the inactive silicon substrate is a bad conductor (K=0), while the 30 nm thin freestanding porous membrane offers negligible background impedance (K = K_{medium} = 1.5 S/m) (Snyder et al. 2013).

Cell growth was modeled using a biphasic growth curve: initial phase of exponential cell growth (3) followed by a stabilizing growth due to contact inhibition (4) (Bindschadler and McGrath 2007).

$$\frac{dN}{dt} = rN \tag{3}$$

$$\frac{dN}{dt} = rN\left(1 - \frac{N}{N_{max}}\right) \tag{4}$$

Initial cell seeding density was 50000 cells/cm^2. Endothelial cells were assumed to have a total surface area of 1000 μm^2 (Jaffe 1987). Thus, the total area occupied by cells was 5x10^7 μm^2 or 0.5 cm^2, and the initial fraction of area occupied by cells was 0.50 or 50%. The cells were simulated to grow without any inhibition until they reach 90% confluence, after which their growth slowed due to contact-inhibition (Bindschadler and McGrath 2007). The final termination density was >97% (represented by 'N_{max}' in Eq. 4). Since the experiments spanned for 14 days, the growth curve was modeled from day zero to day 14, with day zero being the time of initial cell seeding, and the density at day 14 set to be the termination density.

The electrical characteristics of the growing cell monolayer were modeled from the growth curve in accordance with the superposition principle. The cell monolayer was modeled as a 10 micron thick conducting sheet above the membrane. This layer was assigned a spatially uniform conductivity value that varied with the density of cell confluence. This model is consistent with an assumption that cells are perfect insulators and all ionic transport essentially occurs through the gaps (junctions) between cells. The assumption of non-conducting cells is valid, because at low frequency AC, capacitive impedance offered by the lipid bilayer is significantly higher than the junctional resistance (Sun et al. 2010), channeling the electric current through the 'path of least resistance'. Thus, a 20% confluent monolayer rendered a conductivity value of 80% of the bulk media (i.e. K_{cell} = 0.8*K_{medium} = 0.8*1.5 = 1.2 S/m) and, as the cell monolayer grew more confluent, the assigned conductivity of the cell monolayer proportionately decreased and the transmembrane resistance increased.

To reduce the computational complexity of the simulations, time-independent DC simulations were performed. This approximation is valid since the experimental apparatus uses only a very-low frequency (12.5 Hz) AC current. AC prevents the electric corrosion of the silver-silver chloride electrodes used in the EndOhm apparatus. Since the electric simulations are independent of this electrochemical phenomenon, DC current provides a simplified alternative without compromising the accuracy of the simulation output. COMSOL model was validated by comparing experimentally obtained TEER values from transwells filled with solutions of known conductivity to the FEA simulations

with same transwell geometry and identical conductivity solutions. Transwells with 6.5 mm diameter TE membrane (24-well configuration) were used for these studies. The transwells were immersed in the cell media of different dilutions and TEER was measured (n=3). Regular cell media has a conductivity of ∼1.5 S/m, and 2x and 4x dilutions yielded lower conductivity values.

4 Results

4.1 Effects of membrane geometry on resistance: the fallacy of resistance normalization

TEER measurements are very sensitive to the geometry of the membrane and its housing, and to the configuration of electrodes (Srinivasan et al. 2015; ávan der Meer et al. 2015; Henry et al. 2017; Benson et al. 2013). We illustrate this dependance by using transwell inserts of increasing membrane area: 24-, 12-, and 6-well plate transwells. Experiments were done without cellular monolayers to avoid any cell-induced variability. Recommended volumes of cell culture medium were introduced in the transwells and their bottom compartments, and TEER was measured using STX2 chopstick electrodes. The unequal length of chopstick electrodes in apical and basal compartments ensure that the electric field lines bend around the housing, and can 'accommodate' a larger media volume in case of bigger transwells. Thus, STX2 electrodes are useful since they can be used with any size of transwell inserts, unlike EndOhm chambers that are designed for a particular transwell size. The use of the popular chopstick electrodes (rather than the EndOhm chamber), also increases the non-uniformity of field lines for the purposes of this illustration (Figure S1).

In Fig. 2, the dashed red curve represents TEER measurements taken with commercial transwells. As the area of the membrane increases, the product of resistance and the respective membrane area also increases. These resistance values represent 'background' resistances during an actual cell-culture experiment, and typically are subtracted from experimentally measured values to yield the resistance offered by cells only. This background subtraction, however, does not correct for the non-linearities involved in TEER acquisition.

Next, in order to simulate the limited active area seen with silicon nanomembrane chips, we used impermeable silicone gaskets to seal the annular regions of the membrane in the TE-transwell inserts. The annular shape exposed only a fraction of the TE membrane for permeation, and the covered regions were impermeable to ionic transport,

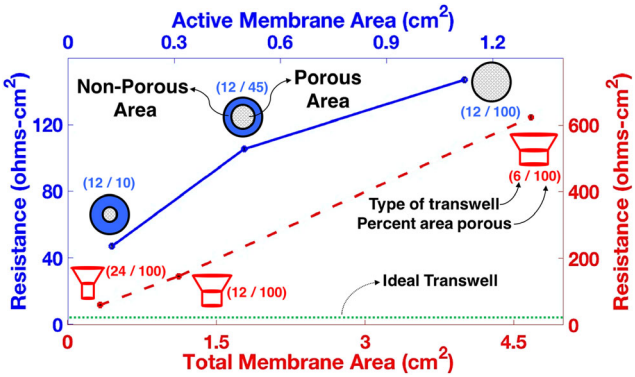

Fig. 2 The graph depicts different transwell configurations used and their TEER values. For e.g., (12,45) indicates a 12-well transwell insert with only 45% area exposed in the center for permeation. Error bars (very small) indicate standard error of mean

mimicking the case for silicon nanomembranes. Even for these 'modified' transwells, the product of resistance and respective membrane area increases with exposed area, but non-linearly in this case, as represented by the solid blue curve in Fig. 2. The dotted green line at the bottom of the plot represents an expected (ideal) outcome of normalizing the decreased resistance values with increasing membrane area.

The results for both conventional and modified transwells can be understood as follows. As the size of the transwell increases, the average path taken by the charge-carrying species from the transmitting electrodes to the receiving electrodes also increases in a non-linear fashion. The geometry of the system is too complex to analytically deduce the changes in path length and verify the increase in resistance values theoretically. The resistance does not decrease with increased cross-sectional area as might be expected for a cable, and the product of resistance and area increases at larger membrane sizes. While the details of this example are particular to the chopstick electrode configuration, it illustrates the need for caution when comparing TEER values between systems even if they are 'normalized' for different areas.

4.2 Development and validation of a FEA model

Since the geometry of the transwell units are too complicated to be analyzed using analytical methods, we employed finite element analysis (FEA) models to study and characterize the electrical behavior of these systems. We used COMSOL for modeling the transwell geometry and FEA. Since our model excludes any time- or frequency-variant component, time-independent simulations were performed

to yield the resistance values. This approach is computationally efficient, and also valid because the experimental measurements were obtained at a very low frequency of 12.5 Hz. The FEA model simulations used 10 μA as an input parameter, and the resultant voltage drop was used to yield the resistance values. The FEA model is shown in Fig. 3a, and results of the validation are shown in Fig. 3b. For all three values of conductivity, the resistance values from the COMSOL simulations matched closely with the ones obtained experimentally.

Having validated the model with TE membranes, we then compared the electrical behavior of TE membranes and nanomembranes under identical input conditions. The nanomembranes also had a total area of ~0.33 cm^2 like TE membranes, but were only permeable through two 2 mm by 0.1 mm wide slots in the center of the chip. Thus, the total active area available for ionic transport was only 0.4 mm^2 in the nanomembrane simulations. Simulation results show that the TE membrane experiences nearly uniform electric field lines that pass orthogonally through the membrane in the EndOhm system (Fig. 4a). This quasi-uniform electrical behavior likely explains the reliability of the EndOhm compared to the STX2 (chopstick) electrodes. By contrast, a simulated nanomembrane-insert resulted in bent field lines that are concentrated at the porous membrane 'windows' (Fig. 4b). The additional path length caused by the field line focusing increases the baseline

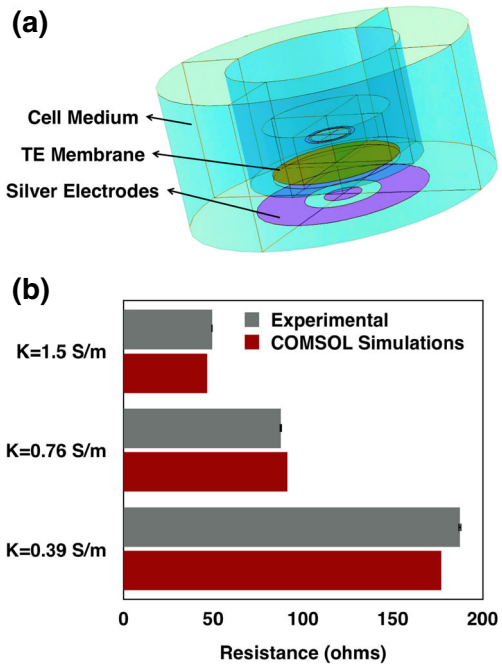

Fig. 3 **a** - COMSOL model of EndOhm chamber with a TE membrane transwell insert inside. **b** - TEER values from experiments compared with simulation results. Cell culture medium of known conductivity was used. Error bars (very small) show standard error of mean [n=3]

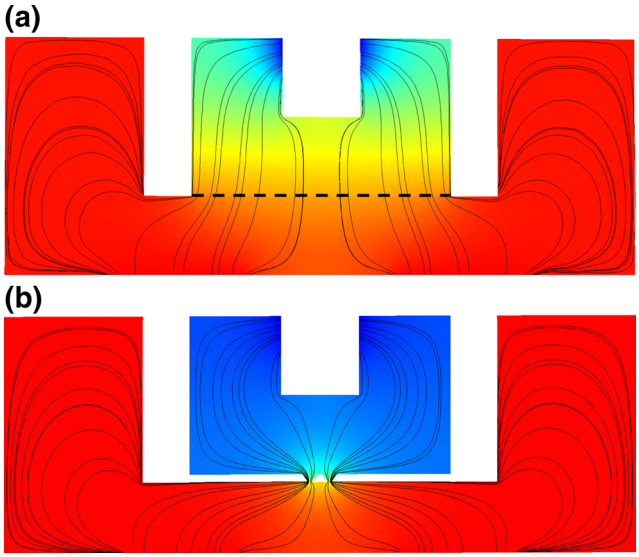

Fig. 4 Simulated electric field lines in the cross-section of EndOhm system for transwell inserts with TE membranes (**a**) and with 2-slot silicon nanomembranes (**b**). The dashed line in (**a**) represents the position of the TE membrane within the system, while the two constricted regions at the similar position in the system represents the active area of silicon nanomembrane in (**b**). The 'squeezing' of electric field lines in the nanomembrane leads to a 10-12X higher baseline resistance as predicted by the COMSOL model

system resistance. Under otherwise identical conditions, simulations predicted a baseline resistance for inserts with 2-slot nanomembranes ~10.8 times higher than the ones with uniform TE membrane.

4.3 Modeling cell growth

To explore how changes in field line behavior translate to TEER values in barrier studies, we cultured brain endothelial (bEnd.3) cells on 2-slot nanomembrane substrates both *in vitro* and *in silico*. Changes in TEER values reflected the growth and maturation of the culture, with resistance values eventually achieving a plateau upon cell confluence. We modeled cell growth kinetics in COMSOL using a contact inhibited logistic growth curve previously developed in our lab (Bindschadler and McGrath 2007). In the electrical model, cell growth was simulated as a layer above the membrane that increases in resistivity over time. Since the COMSOL data simulates the same cell-growth phenomena on two different membrane systems, we can use the predictions from each system to convert TEER values from one system to the other. In this way TEER values obtained on nanomembranes in a microdevice can be 'corrected' to enable comparisons to TEER values obtained by others on TE membranes in transwell devices.

Brain endothelial (bEnd.3) cells were cultured in the transwells fitted with either silicon nanomembranes or with

polymer TE membranes. Baseline resistance values were measured in both the systems before initial cell seeding. In COMSOL simulations, cell-growth was represented by the changes in the conductivity of the cell layer, K_{cell}, which was calculated from the degree of confluence, c, according to: $K_{cell} = (1\text{-}c)*K_{medium}$, where K_{medium} is the bulk media conductivity, and $0 < c < 1$. This effectively assumes the growing cell layer is a superposition of insulators (cells) and resistors (media between the cells) with the degree of confluence equal to the ratio of cell-occupied area to the total area. This superposition principle is valid because cell membranes act as insulating capacitors at low frequency AC (Sun et al. 2010), and the electric current essentially flows through paracellular gaps. We assume that a perfect monolayer (100% confluent) is not achievable since this would give an open circuit and therefore we must use the maximum confluence value as a free parameter in each model fit. With this addition to the EndOhm model developed and validated earlier, we accurately predicted the increases in TEER values on the both membrane systems (Fig. 5; RMS errors of 7% for TE membranes and 9% for silicon membranes).

The terminal TEER values obtained here (~13 Ω-cm^2) are much lower than the published values for blood brain barrier (BBB) (>100 Ω-cm^2) (Booth and Kim 2012), but this difference is not due to the geometry or the nature of the membrane used for culturing brain endothelial cells, since the corrected values on both TE and nanomembranes are identical. Instead we note that, BBB typically needs the growth of brain endothelial cells under physiological levels of shear stress (>10 dynes/cm^2), and needs to be cocultured with astrocytes and pericytes for enhanced barrier properties (Booth and Kim 2012). This has motivated us to develop a more comprehensive nanomembrane microsystem for vascular mimetics, which we will introduce in forthcoming publications.

4.4 Mapping function

To obtain a mapping function between the two membranes we used 'number of days in culture' as an independent parameter in a plot of TEER values for silicon and TE membranes (Fig. 5). The results show a local non-linearity that can be best understood from a plot of the ratio of simulated resistance values for the nanomembrane to the TE membrane (Fig. 6a). Here, we see that the ratio (R_{nano} : R_{TE}) is initially ~11 and returns to a similar value once both monolayers become confluent. The intermediate increase in the ratio is likely due to the fact that the cells are growing at slightly different rates on the two materials. We have previously shown that endothelial cells grow slightly faster on nanomembranes compared to polymeric substrates (0.0296 divisions/cell-hour for silicon membranes vs 0.0223 divisions/cell-hour for polymer substrates) (Agrawal et al. 2010). The more rapid achievement of a TEER plateau value on nanomembranes (3-5 days) compared to TE membranes (5-7 days) is consistent with this earlier finding. Thus, we do not believe that the different dynamics during the logistic growth phase are due to the electrical behavior of the two membranes.

Once the cells have reached confluence, both systems act as a series of resistors, where the only difference is attributed to the membrane geometry (Fig. 6c). Hence, the mapping, or the correction function, is simply a line (Fig. 6a dashed line), whose ordinate (Y) intercept is equal to the ratio of the plateau resistances of the two systems. Because this ratio is a function of the membrane geometry and electrode positioning, a different configuration of these variables would require a new FEA simulation to obtain a new ratio. In this case, the ratio is 11.4 and hence, if one wishes to report 2-slot nanomembrane TEER values as equivalent TEER values on a commercial 24 well TE insert, one would first divide the nanomembrane value by 11.4 and

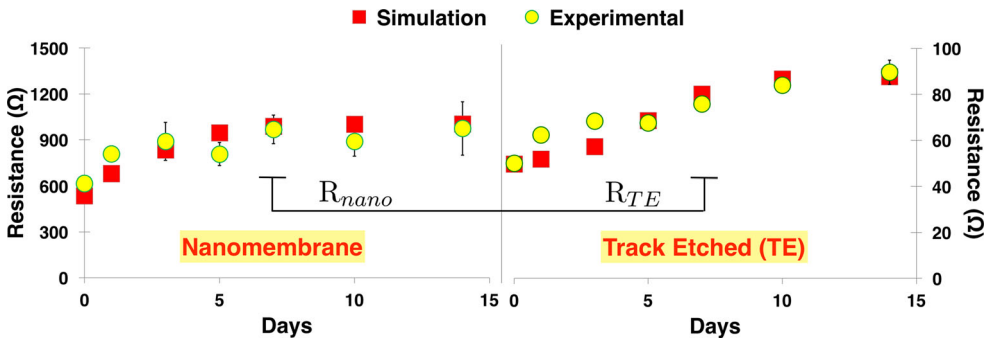

Fig. 5 Experimental (yellow circles) vs simulation (red squares) results demonstrating the increase in TEER during bEnd.3 cell growth on silicon nanomembrane and on TE membranes. Note the difference in the magnitude of the measured resistances, although both experimental curves follow a similar trend. Error bars represent standard error of mean [n=3-5]. The ratio of simulated resistances (R_{nano} : R_{TE}) is calculated by dividing the resistance from nanomembrane on a given day (for e.g. day 7, as shown in the figure) to the resistance obtained from TE membrane on the same day (i.e. day 7 in this case). This ratio is used to create a mapping function between the two systems (refer Fig. 6 and Section 4.4)

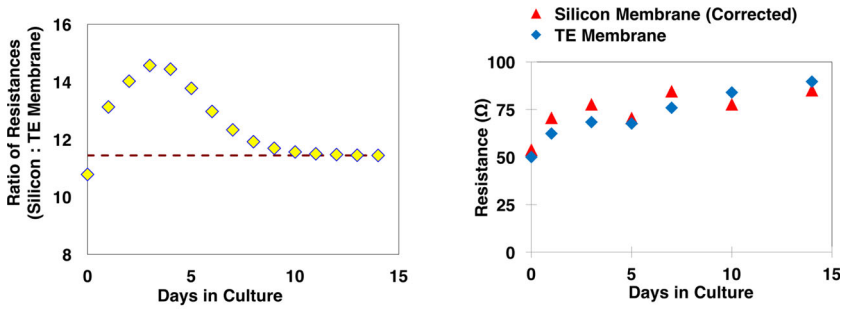

(a) Ratio of resistance (Nano:TE) **(b)** Overlap of the mapped data

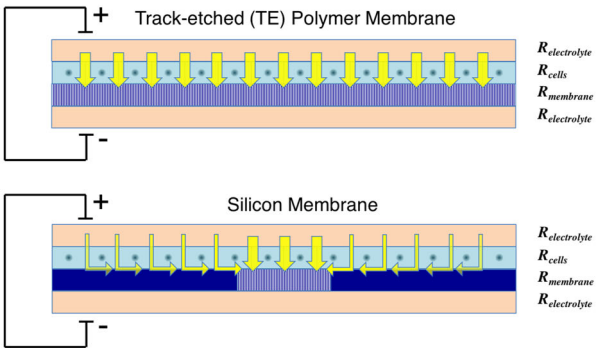

(c) Difference in electric field lines in confluent systems

Fig. 6 **a** - The ratio of resistances obtained from COMSOL simulation for the two membranes. Note that the ratio is dynamic during the intermediate phases of growth due to different growth rates on different substrates, but plateaus as the cells reach confluence. The plateauing value of ratio (11.4 in this case) reflects the difference in the geometry of the two systems, and can be used to convert TEER values from nanomembrane to TE membranes equivalents. **b** - Resistance values obtained from silicon membrane are corrected by dividing with 11.4 to yield the corrected values, which match well with the values from TE membranes. **c** - The schematic demonstrates the spatial distribution and intensity of the electric field through the confluent monolayer of cells on different systems. The effective path length and the cross sectional area approach a constant value for the systems as cells reach confluence, and the resistances can be linked together through a simple multiplicative constant

then multiply by the area of a 24 well insert (0.33 cm^2), to obtain the conventional transwell value in ohms-cm^2. Once the conversion is completed, background subtraction needs to be performed to yield cellular resistances only (Online Resource 2). Figure 6b compares the corrected resistance values (using the mapping function) for cell growth on nanomembranes to those on TE membranes. The two curves match very closely, with a RMS error of ∼8%.

5 Discussion

Intact barrier tissues are important for homeostasis and normal functioning of all organs including skin, lungs, gastrointestinal (GI) tract, kidney, retina and brain (Sakolish et al. 2016). Damage or loss of integrity of these barrier properties can be responsible for multiple degenerative and fatal disorders. Loss of intact blood-brain-barrier (BBB) due to excessive infiltration of immune cells in the brain is responsible for disorders such as multiple sclerosis (Pinheiro et al. 2016). Systemic inflammatory conditions like septic shock disrupts microvascular barrier function leading to excessive fluid loss and increased patient mortality (Lee and Slutsky 2010; Acheampong and Vincent 2015). Disruption of barrier tissues in lungs can lead to increased extravasation of neutrophils in bronchial spaces causing chronic obstructive pulmonary disorder (COPD) (Woolhouse et al. 2005). Thus, it is extremely important to understand the organ- and tissue-specific physiology of the barrier tissues for a more targeted clinical intervention (Sakolish et al. 2016). Development of *in vitro* platforms that can accurately capture the pathophysiology of the barrier tissues will be an important step towards the discovery, development, and delivery of therapeutic drugs (Bhatia and Ingber 2014). Towards this end, development of micro-physiological systems (MPS) serve as a promising platform to model and study human pathological conditions (Sutherland et al. 2013).

A variety of MPS are used to model different organ specific tissue barriers including the brain (Walter et al. 2016; Booth and Kim 2012; Cucullo et al. 2013), GI tract (Kim et al. 2012), lung (Huh et al. 2012), microvessel (Bogorad et al. 2015; Vogel et al. 2011) etc. Most of these *in vitro* models of barrier tissues employ a

porous membrane for coculture of relevant cell types. Commercially available systems featuring track etched (TE) membranes suffer significant limitations including 1) *aphysiological* barrier thicknesses (~10 microns), 2) poor phase imaging quality and autofluorescence, 3) low porosity (pore:cell ratios <1) and permeability, and 4) challenges with microsystem integration. In contrast, silicon nanomembranes developed over the last decade are extremely thin, highly permeable, offer superior imaging characteristics, and are manufacturable in large quantities (Striemer et al. 2007; DesOrmeaux et al. 2014).

The permeability of membranes used for coculturing plays an important role in the differentiation of growing cells to mimic *in vivo* functions (Ryu et al. 2015; Mazzocchi et al. 2014). The ultrathin nature of silicon nanomembranes makes them ideal for proximal coculture applications and for modeling barrier tissues *in vitro* (Agrawal et al. 2010; Carter et al. 2017). In the past, we have demonstrated the advantages of using silicon nanomembranes over commercially available TE membranes for a variety of biological applications including vasculogenesis (Nehilla et al. 2014), stem cell differentiation (Mazzocchi et al. 2014), shear-free chemotaxis of leukocytes (Chung et al. 2014) and hemodialysis (Johnson et al. 2013). The nanometer thickness renders negligible diffusive resistances to small molecules (Snyder et al. 2013) - a characteristic that should enhance paracrine signaling in cocultures (Carter et al. 2017). The advantages that nanomembranes have for studying cell barriers, including multi-cellular layers, motivate the present analysis so that TEER measurements can be reliably understood and interpreted for cell layers grown using nanomembrane platforms.

Electrical methods of characterizing tissue permeability have been used for over 60 years in different animal models. These methods provide better temporal resolution over chemical methods because they depend on the instantaneous mobilities of the ionic species across the barrier structure instead of much slower diffusion of the macromolecular fluorescent markers. The pioneering work on using electrical measurements to assess tissue barrier function was published by Hans Ussing in the 1950's in his studies on the transport properties of frog epithelium. Subsequently, using slightly different principles, Crone and colleagues, in the early 1980s, successfully measured the ionic conductances in the BBB of a live frog, establishing the gold standard for TEER values in brain microvasculature (Crone and Christensen 1981; Crone and Olesen 1982). Presently, hanging bucket transwell systems, inspired from the Boyden chambers, are the most popular systems used for barrier studies because of their ease of use, and are routinely used in combination with STX2 'chopstick' electrodes for TEER measurement [WPI Inc., Sarasota, FL]. Unfortunately, this method of TEER measurement is subject to artifactual differences in measured values because of differences in the size of the transwells that are used, and the precise placement of the electrodes. To compare the TEER values obtained from *in vitro* setups (in Ω) to *in vivo* values (in Ω-cm^2), and the desire to standardize measurements across different *in vitro* systems, resistances are multiplied with membrane area. While this convention has been widely adopted for decades, it can be flawed. A simple experiment presented in Fig. 2 illustrates that the product of resistance and the membrane area increases monotonically with area - a clear sign that the multiplication does not constitute a proper normalization of the measurements. Online Resource 1 demonstrates the non-uniformity of the field lines with chopstick electrodes. Our attempts to apply these same corrections to silicon nanomembranes with very small active areas revealed even more problematic discrepancies. Confronted with this paradox, we sought a computational model to help us rationalize the differences between the two systems.

The past decade witnessed a growth in the use of microfluidic systems as barrier tissue models (Vogel et al. 2011; Douville et al. 2010; Booth and Kim 2012; Booth et al. 2014; Walter et al. 2016; Ferrell et al. 2010; ávan der Meer et al. 2015; Henry et al. 2017; Wang et al. 2017). As these microsystems have become more sophisticated, relatively little attention has been paid to underlying assumptions in permeability measurements. While the *in vitro* systems fail to match the physiological complexity of the *in vivo* environment, making meaningful comparisons between any two systems is not as simple as multiplying resistance by membrane area (Srinivasan et al. 2015).

Research groups developing microsystems for barrier models have taken different approaches for the interpretation of TEER values. One recent study designed their microsystem to match the shape of the commercially available 6.5 mm wide transwell insert (Wang et al. 2017). The rationale behind this approach is to obtain similar TEER values as observed in the commercial system, which will allow the researchers to directly multiply the resistance values with the membrane area, and make it easy to compare them against the published TEER values in the literature. Although sound, this obviously limits the design and applications of the microsystem. Another study developed a mapping function for their system to interpret the raw resistance values using finite element analysis (ávan der Meer et al. 2015). Our work provides a generalizable modeling approach, which can be developed, verified, and applied to compare resistance values between *any* customized microsystem (see Online Resource 2). FEA modeling of microsystems not only allows the user to understand the electric behavior, but also reveals opportunities to optimize for more sensitive and reliable TEER measurements. For instance, current efforts in our lab are focused

on developing microsystems with integrated patterned electrodes, and the FEA modeling is able to predict the raw resistance values observed experimentally.

Many prior studies have employed FEA tools to understand the electrical behavior of cells in customized microsystems (Sun et al. 2010; Tandon et al. 2010; Yeste et al. 2015). Our own analysis demonstrated the utility of the FEA model in multiple ways. First, we were able to accurately simulate the electrical behavior in the EndOhm system in the absence of the cells in COMSOL Multiphysics by using media of different conductivity values (Fig. 3) as seen elsewhere (Wang et al. 2017). The close match between the experiment and simulation also established the validity of using simpler time-independent DC simulations to model low frequency AC experiments. Next, we modeled a growing cellular layer using a modified logistic growth curve (Bindschadler and McGrath 2007) to model the evolution of TEER values with time. Interestingly, we have shown that endothelial cells grow faster on silicon nanomembranes compared the polymer substrates (Agrawal et al. 2010) and a similar phenomenon can be observed here with a faster rise of our TEER data (Fig. 6b). TEER values eventually stabilize at a plateau in both systems (4-5 days on silicon nanomembranes; >one week on TE membranes) (Fig. 5). Assuming the cells achieve the same resistant monolayer on both systems, the ratio of the plateau values is the transfer function between the two systems that can be used to relate TEER values as a measure of barrier function. The final ratio of resistances differs slightly from the initial ratio (Fig. 6a) indicating that the cell layer slightly affects the field lines through the membrane. Using the percentage confluence as the only floating parameter, we were able to predict the end-point TEER values with less than 10% RMS error.

6 Conclusion

We have successfully employed a computational model to understand the electrical response of transwell inserts with different membrane geometries. This development is important to the application of nanomembranes for the creation of barrier models where their optical transparency and ultrathin nature have advantages over conventional systems. The model provided the necessary function to convert the resistance value from silicon nanomembrane transwell microsystem to conventional TE membrane inserts enabling us to supermpose the two datasets. Although these results are specific to 2-slot silicon nanomembranes, the modeling approach can be easily extended to different membrane geometries and device configurations. The development of a mapping function provides an unique and reliable algorithm to interpret and compare the TEER values across different platforms.

Acknowledgements Authors would like to thank Dr. Henry Chung, Zachery Hulings and Tucker Bergin for their help in COMSOL modeling, and Thomas Andolsek in obtaining the TEER data for validation experiments. They also acknowledge the support of Dr. Allison Elder (Department of Environmental Medicine, University of Rochester) during the early days of this project. This work was supported by funding from the National Institutes of Health under program project grant number: 5 R01 HL125265.

References

A. Acheampong, J.-L. Vincent, A positive fluid balance is an independent prognostic factor in patients with sepsis. Crit. Care **19**(1), 251 (2015)

A.A. Agrawal, B. Nehilla, K. Reisig, T. Gaborski, D. Fang, C. Striemer, P. Fauchet, J. McGrath, Porous nanocrystalline silicon membranes as highly permeable and molecularly thin substrates for cell culture. Biomaterials **31**(20), 5408–17 (2010)

A.D. ávan der Meer, H. JungáKim, M.W. ávan der Helm, A. den Berg, Measuring direct current trans-epithelial electrical resistance in organ-on-a-chip microsystems. Lab Chip **15**(3), 745–52 (2015)

K. Benson, S. Cramer, H.-J. Galla, Impedance-based cell monitoring: Barrier properties and beyond. Fluids Barriers CNS **10**(1), 5 (2013)

S.N. Bhatia, D.E. Ingber, Microfluidic organs-on-chips. Nat. Biotechnol. **32**(8), 760–72 (2014)

M. Bindschadler, J.L. McGrath, Sheet migration by wounded monolayers as an emergent property of single-cell dynamics. J. Cell Sci. **120**(5), 876–84 (2007)

M.I. Bogorad, J. DeStefano, J. Karlsson, A.D. Wong, S. Gerecht, P.C. Searson, *in vitro* microvessel models. Lab Chip **15**(22), 4242–55 (2015)

R. Booth, H. Kim, Characterization of a microfluidic *in vitro* model of the blood-brain barrier (μbbb). Lab Chip **12**(10), 1784–92 (2012)

R. Booth, S. Noh, H. Kim, A multiple-channel, multiple-assay platform for characterization of full-range shear stress effects on vascular endothelial cells. Lab Chip **14**(11), 1880–90 (2014)

R.N. Carter, S.M. Casillo, A.R. Mazzocchi, J.-P.S. DesOrmeaux, J.A. Roussie, T.R. Gaborski, Ultrathin transparent membranes for cellular barrier and co-culture models. Biofabrication **9**(1), 015,019 (2017)

S.M. Casillo, A.P. Peredo, S.J. Perry, H.H. Chung, Gaborski T. R, Membrane pore spacing can modulate endothelial cell–substrate and cell–cell interactions. ACS Biomaterials Sci. Eng. (2017)

H.H. Chung, C.K. Chan, T.S. Khire, G.A. Marsh, A. Clark, R.E. Waugh, J.L. McGrath, Highly permeable silicon membranes for shear free chemotaxis and rapid cell labeling. Lab Chip **14**(14), 2456–68 (2014)

C. Crone, O. Christensen, Electrical resistance of a capillary endothelium. J. Gen. Physiol. **77**(4), 349–71 (1981)

C. Crone, S. Olesen, Electrical resistance of brain microvascular endothelium. Brain Res. **241**(1), 49–55 (1982)

L. Cucullo, M. Hossain, W. Tierney, D. Janigro, A new dynamic *in vitro* modular capillaries-venules modular system: cerebrovascular physiology in a box. BMC Neurosci. **14**(1), 18 (2013)

J. DesOrmeaux, J. Winans, S. Wayson, T. Gaborski, T. Khire, C. Striemer, J. McGrath, Nanoporous silicon nitride membranes fabricated from porous nanocrystalline silicon templates. Nanoscale **6**(18), 10,798–805 (2014)

N.J. Douville, Y.-C. Tung, R. Li, J.D. Wang, M.E. El-Sayed, S. Takayama, Fabrication of two-layered channel system with embedded electrodes to measure resistance across epithelial and endothelial barriers. Anal. Chem. **82**(6), 2505 (2010)

R.S. Eisenberg, E.A. Johnson, Three-dimensional electrical field problems in physiology. Prog. Biophys. Molecul. Biol. **20**, 1–65 (1970)

N. Ferrell, R.R. Desai, A.J. Fleischman, S. Roy, H.D. Humes, W.H. Fissell, A microfluidic bioreactor with integrated transepithelial electrical resistance (teer) measurement electrodes for evaluation of renal epithelial cells. Biotechnol. Bioeng. **107**(4), 707–16 (2010)

O. Henry, R. Villenave, M. Cronce, W. Leineweber, M. Benz, D. Ingber, Organs-on-chips with integrated electrodes for trans-epithelial electrical resistance (teer) measurements of human epithelial barrier function. Lab Chip (2017)

D. Huh, D.C. Leslie, B.D. Matthews, J.P. Fraser, S. Jurek, G.A. Hamilton, K.S. Thorneloe, M.A. McAlexander, D.E. Ingber, A human disease model of drug toxicity–induced pulmonary edema in a lung-on-a-chip microdevice. Sci. Translat. Med. **4**(159), 159ra147–159ra147 (2012)

R. Ishimatsu, J. Kim, P. Jing, C.C. Striemer, D.Z. Fang, P.M. Fauchet, J.L. McGrath, S. Amemiya, Ion-selective permeability of an ultrathin nanoporous silicon membrane as probed by scanning electrochemical microscopy using micropipet-supported ities tips. Anal. Chem. **82**(17), 7127–34 (2010)

E.A. Jaffe, Cell biology of endothelial cells. Human Pathol. **18**(3), 234–9 (1987)

D.G. Johnson, T.S. Khire, Y.L. Lyubarskaya, K.J. Smith, J.-P.S. DesOrmeaux, J.G. Taylor, T.R. Gaborski, A.A. Shestopalov, C.C. Striemer, J.L. McGrath, Ultrathin silicon membranes for wearable dialysis. Adv. Chronic Kidney Dis. **20**(6), 508–15 (2013)

L.C. Kelley, L.L. Lohmer, E.J. Hagedorn, D.R. Sherwood, Traversing the basement membrane *in vivo*: A diversity of strategies. J. Cell. Biol. **204**(3), 291–302 (2014)

H.J. Kim, D. Huh, G. Hamilton, D.E. Ingber, Human gut-on-a-chip inhabited by microbial flora that experiences intestinal peristalsis-like motions and flow. Lab Chip **12**(12), 2165–74 (2012)

W.L. Lee, A.S. Slutsky, Sepsis and endothelial permeability. England J. Med. **363**(7), 689 (2010)

A.R. Mazzocchi, A.J. Man, J.-P.S. DesOrmeaux, T.R. Gaborski, Porous membranes promote endothelial differentiation of adipose-derived stem cells and perivascular interactions. Cell. Mol. Bioeng. **7**(3), 369–78 (2014)

B.J. Nehilla, N. Nataraj, T.R. Gaborski, J.L. McGrath, Endothelial vacuolization induced by highly permeable silicon membranes. Acta Biomaterialia **10**(11), 4670–7 (2014)

M.A.L. Pinheiro, G. Kooij, M.R. Mizee, A. Kamermans, G. Enzmann, R. Lyck, M. Schwaninger, B. Engelhardt, H.E. de Vries, Immune cell trafficking across the barriers of the central nervous system in multiple sclerosis and stroke. Biochimica et Biophysica Acta (BBA)-Molecular Basis Disease **1862**(3), 461–71 (2016)

S. Ryu, J. Yoo, Y. Jang, J. Han, S.J. Yu, J. Park, S.Y. Jung, K.H. Ahn, S.G. Im, K. Char, Nanothin coculture membranes with tunable pore architecture and thermoresponsive functionality for transfer-printable stem cell-derived cardiac sheets. ACS Nano **9**(10), 10,186–202 (2015)

C.M. Sakolish, M.B. Esch, J.J. Hickman, M.L. Shuler, G.J. Mahler, Modeling barrier tissues *in vitro*: Methods, achievements, and challenges. EBioMedicine **5**, 30–9 (2016)

J. Seok, H.S. Warren, A.G. Cuenca, M.N. Mindrinos, H.V. Baker, W. Xu, D.R. Richards, G.P. McDonald-Smith, H. Gao, L. Hennessy, Genomic responses in mouse models poorly mimic human inflammatory diseases. Proc. Natl. Acad. Sci. **110**(9), 3507–12 (2013)

J. Snyder, A. Clark, D. Fang, T. Gaborski, C. Striemer, P. Fauchet, J. McGrath, An experimental and theoretical analysis of molecular separations by diffusion through ultrathin nanoporous membranes. J. Membrane Sci. **369**(1), 119–29 (2011)

J.L. Snyder, J. Getpreecharsawas, D.Z. Fang, T.R. Gaborski, C.C. Striemer, P.M. Fauchet, D.A. Borkholder, J.L. McGrath, High-performance, low-voltage electroosmotic pumps with molecularly thin silicon nanomembranes. Proc. Nat. Acad. Sci. **110**(46), 18,425–30 (2013)

B. Srinivasan, A.R. Kolli, M.B. Esch, H.E. Abaci, M.L. Shuler, J.J. Hickman, Teer measurement techniques for *in vitro* barrier model systems. J. Laborat. Autom. **20**(2), 107–26 (2015)

C.C. Striemer, T.R. Gaborski, J.L. McGrath, P.M. Fauchet, Charge-and size-based separation of macromolecules using ultrathin silicon membranes. Nature **445**(7129), 749–53 (2007)

T. Sun, E.J. Swindle, J.E. Collins, J.A. Holloway, D.E. Davies, H. Morgan, On-chip epithelial barrier function assays using electrical impedance spectroscopy. Lab Chip **10**(12), 1611–7 (2010)

M.L. Sutherland, K.M. Fabre, D.A. Tagle, The national institutes of health microphysiological systems program focuses on a critical challenge in the drug discovery pipeline. Stem Cell Res. Therapy **4**(1), I1 (2013). https://doi.org/10.1186/scrt361

N. Tandon, A. Marsano, R. Maidhof, K. Numata, C. Montouri-Sorrentino, C. Cannizzaro, J. Voldman, G. Vunjak-Novakovic, Surface-patterned electrode bioreactor for electrical stimulation. Lab Chip **10**(6), 692–700 (2010)

K. Tanner, Regulation of the basement membrane by epithelia generated forces. Phys. Biol. **9**(6), 065,003 (2012)

P.A. Vogel, S.T. Halpin, R.S. Martin, D.M. Spence, Microfluidic transendothelial electrical resistance measurement device that enables blood flow and postgrowth experiments. Anal. Chem. **83**(11), 4296–301 (2011)

F.R. Walter, S. Valkai, A. Kincses, A. Petneházi, T. Czeller, S. Veszelka, P. Ormos, M.A. Deli, A. Dér, A versatile lab-on-a-chip tool for modeling biological barriers. Sens. Actuators B **222**, 1209–19 (2016)

Y.I. Wang, H.E. Abaci, M.L. Shuler, Microfluidic blood–brain barrier model provides *in vivo*-like barrier properties for drug permeability screening. Biotechnol. Bioeng. **114**(1), 184–94 (2017)

I. Woolhouse, D. Bayley, P. Lalor, D. Adams, R. Stockley, Endothelial interactions of neutrophils under flow in chronic obstructive pulmonary disease. Europ. Respir. J. **25**(4), 612–7 (2005)

J. Yeste, X. Illa, A. Guimerà, R. Villa, A novel strategy to monitor microfluidic in-vitro blood-brain barrier models using impedance spectroscopy. In: SPIE Microtechnologies, International Society for Optics and Photonics, pp. 95,180N–95,180N (2015)